

Cohesins Bind to Preferential Sites along Yeast Chromosome III, with Differential Regulation along Arms versus the Centric Region

Yuval Blat* and Nancy Kleckner
Department of Molecular and Cellular Biology
Harvard University
Cambridge, Massachusetts 02138

Summary

Sister chromatid cohesion is mediated by evolutionary conserved chromosomal proteins, termed “cohesins.” Using an extension of chromatin immunoprecipitation, we have analyzed the distribution of cohesins Mcd1/Scc1 and Smc1 along yeast chromosome III. Both proteins occur preferentially at the same ~23 positions. Sites in a ~50 kb region around the centromere give especially intense signals. Prominent centric region binding appears to emerge from a more even distribution, probably by differential loss of cohesins along the chromosome arms. Cohesin binding peaks correspond closely to peaks of high local AT composition, a base composition periodicity of ~15 kb that is distinct from the ~50 kb periodicity of base composition isochores, consistent with axis association of cohesins. The methodology described can be used to analyze the distribution of any DNA-binding protein and, via microchips, along entire genomes.

Introduction

Sister chromatid cohesion is an essential component of chromosome organization and is necessary for regular disjunction of chromosomes at anaphase (for reviews, Miyazaki and Orr-Weaver, 1994; Biggins and Murray, 1998). Cohesion arises concomitant with DNA replication and is lost during chromosome segregation at anaphase (Selig et al., 1992; Guacci et al., 1997; Michaelis et al., 1997).

Two interrelated aspects of sister cohesion are particularly interesting: first, sister chromatid cohesion appears to be lost in stages; second, centric regions and arm regions exhibit differential behavior.

At the metaphase/anaphase transition of mitosis, sister chromatid chromatin masses spring apart along the lengths of the chromatid arms, suddenly and independent of spindle forces; wide splitting in centromeric regions then also occurs, closely followed by movement of centromeres toward the poles (Bajer and Mole-Bayer, 1972; Nicklas, 1988). Meiotic chromosomes behave analogously except that the two phases occur at the two successive meiotic divisions (Miyazaki and Orr-Weaver, 1994).

Arms and centric regions exhibit an analogous differential response to microtubule depolymerization agents. Such treatment initially yields chromosomes that are separated along the arms but still connected in centric

regions; eventually, however, centric regions may separate, yielding sister chromatid “ski pairs” (Mole-Bajer, 1958; reviewed in Miyazaki and Orr-Weaver, 1994).

It has been suggested that wide splitting of sisters at metaphase/anaphase is preceded by a minimization of sister connections during mitotic prophase (e.g., concomitant with higher order compaction) (Hirano, 1995; Kleckner, 1996).

Interestingly, also, connections appear to remain between sister chromatid arms even after wide splitting. During mitosis, sister chromatin masses initially remain side by side and then finally “peel apart” progressively, from centromere-proximal regions outward along the arms, concomitant with poleward movement (e.g., Bajer and Mole-Bayer, 1972; E. D. Salmon, personal communication). Scanning electron microscopy images of trypsin-treated mouse chromosomes exhibit signs of late, noncentric connections (Sumner, 1991). During meiosis, pulling-sensitive sister connections are inferred to be present along the lengths of the chromosome arms after the metaphase/anaphase transition because sister connections persist at late anaphase I specifically in arm regions that were never under tension during homolog separation (Maguire, 1995; Kleckner, 1996).

Sister chromatid cohesion is mediated in part by a set of proteins that are highly conserved through evolution. Genetic screens in *S. cerevisiae* for mutations causing an increased rate of chromosome loss or defects in maintenance of sister chromatid cohesion in the presence of the microtubule polymerization inhibitor, nocodazole, identified *MCD1/SCC1*, *SCC2*, *SCC3*, *SMC1*, *SMC3*, and *CTF7/ECO1* (Strunnikov et al., 1993; Guacci et al., 1997; Michaelis et al., 1997; Skibbens et al., 1999; Toth et al., 1999). Homologous genes with similar functions were also identified in *S. pombe* (Birkenbihl and Subramani, 1995; Furuya et al., 1998), and homologs of these genes have been found also in humans and other vertebrates (Guacci et al., 1997; Michaelis et al., 1997; Losada et al., 1998; Toth et al., 1999).

In *S. cerevisiae*, the four proteins Mcd1/Scc1, Scc3, Smc1, and Smc3, termed “cohesins,” appear to form a functional complex that mediates sister chromatid cohesion (Toth et al., 1999), both along chromosome arms and around centromeres (Guacci et al., 1997). Similarly, in *Xenopus* egg extracts, a complex containing five proteins is required for sister chromatid cohesion in vitro; three of which are homologs of Smc1, Smc3, and Mcd1/Scc1 (Losada et al., 1998). Yeast Scc2 is not an integral part of the cohesins complex but is required for the localization of the complex to chromosomes. Ctf7/Eco1 appears to be required during the establishment of cohesion, but not for localization of cohesins to chromosomes (Skibbens et al., 1999; Toth et al., 1999).

Immunolocalization and chromosome fractionation experiments suggest that cohesins load onto the chromosomes prior to, or at the beginning of, DNA replication and, in “well spread” nuclei, form >100 foci (Michaelis et al., 1997; Losada et al., 1998; Uhlmann and Nasmyth,

*To whom correspondence should be addressed (e-mail: blat@fas.harvard.edu).

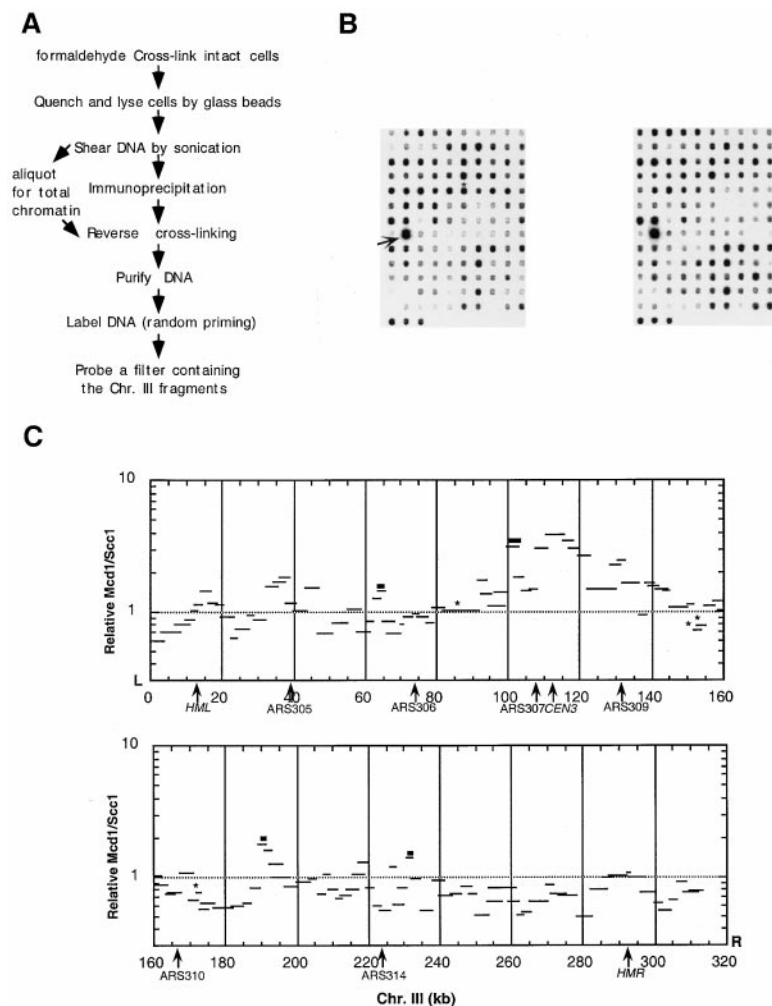


Figure 1. The Distribution of Mcd1/Scc1 in a Logarithmic Culture

(A) A flow chart describing our experimental system.

(B) Chromosome III fragments containing filters probed with immunoprecipitated Mcd1/Scc1-bound DNA (left) or total DNA (right). DNA was immunoprecipitated from a logarithmic culture of YBY92. Fragment order is from the left telomere (top left corner) to near the right telomere (bottom). A fragment containing a full-length Ty element is indicated by an arrow. The fragment containing the minimal centromere fragment is indicated by a star.

(C) A quantitation of the results showed in (B). Every fragment is represented by a bar spanning its entire length. Four regions in which Mcd1/Scc1 binding could be confined to a 1-2 kb are indicated by bold lines. Fragments containing Ty element sequences in either the W303 or the SK-1 background are indicated by a star (these fragments usually give intense signal most of which result probably from sequences outside of chromosome III). See also Baudat and Nicolas (1997) for more information about the strains. Fragment lengths, in case differences exist, reflect the situation in the W303 background.

1998; Toth et al., 1999). Establishment of effective intersister connections is intimately linked to the replication process, temporally and/or functionally (Furuya et al., 1998; Uhlmann and Nasmyth, 1998; Skibbens et al., 1999). Cohesins remain on the chromosomes until the time of chromosome segregation, whereupon at least much of the protein is removed (Michaelis et al., 1997).

Sister chromatids are known to be connected by topological interlinks, and full sister separation requires topoisomerase II activity; whether interlinks are involved in establishment of sister chromatid cohesion and/or faithful sister separation remains to be determined (Miyazaki and Orr-Weaver, 1994).

We were interested to know how cohesins interact with chromosomes with regard to the sequence of the DNA and the overall organization of the chromosomes, and whether/how these features change during chromosome morphogenesis. We report here the analysis of cohesin distribution along an entire yeast chromosome (III) using an extension of chromatin immunoprecipitation (ChIP). Cohesins bind preferentially to genetically defined positions along the chromosomes, with increased abundance in and around the centromere, and with differential behaviors of centric and arm regions as the cell cycle progresses.

In the course of this analysis, we also found that AT/GC composition oscillates regularly, along the chromosome, with periodicity of about 15 kb, in correlation with cohesin binding. This periodicity likely corresponds to the AT-queue of the chromosome axis (Saitoh and Laemmli, 1993). Yeast chromosomes also exhibit a larger ~50 kb periodicity of base composition isochores (Sharp and Lloyd, 1993; Dujon, 1996) that are likely analogous to the R and G bands of mammalian chromosomes. We suggest that these two features contribute combinatorially to structural and functional organization along chromosome arms.

Results

The Experimental System

To monitor the relative distribution of cohesins, or any other chromosomal protein of interest, along a whole yeast chromosome, we modified existing protocols for chromatin immunoprecipitation (Hecht et al., 1996) so that the immunoprecipitated DNA can be radiolabeled and used as a probe in a hybridization experiment rather than, as in the standard protocol, as a template for PCR. ChIP probe is hybridized to a membrane containing an

array of DNA fragments representing chromosomal regions of interest, under conditions of array DNA excess. The relative levels of hybridization observed for different fragments reflect the relative abundance of the chromosome-bound cohesin at the different corresponding regions.

We analyzed the distributions of the cohesins Mcd1/Scc1 and Smc1 along a set of fragments that span the entire length of chromosome III of *S. cerevisiae* (excluding ~1.5–2 kb at each end). Each protein of interest was Myc epitope- or HA epitope-tagged to facilitate immunoprecipitation. Chromosome III was chosen because of its manageable size (315 kb) and because the locations of replication origins, silenced regions, and meiosis-specific double-strand breaks are all known (Newlon et al., 1993; Baudat and Nicolas, 1997). The DNA array comprised 133 PCR-generated fragments, each ~3 kb in length. To ensure a complete view of the chromosome, these fragments include the entire chromosomal sequence, in contrast to other DNA fragment arrays in which only the open reading frames are represented (e.g., DeRisi et al., 1997). For achieving this complete representation with commercially available, well-characterized DNA primers, it was necessary that the sequence of each fragment overlapped at its termini with fragments representing adjacent positions on the chromosome (median degree of overlap between adjacent fragments, 480 bp).

In a typical experiment (Figure 1A), a 1 l culture containing 1–2 10^{10} yeast cells expressing the epitope-tagged protein of interest was subjected to formaldehyde cross-linking. After collection by centrifugation, cells were lysed by glass beads, and DNA was sheared by sonication (average size ~500 bp, range 100–2000 bp). Protein-bound DNA was obtained via immunoprecipitation with tag-specific antibody, purified, radiolabeled by random priming, and hybridized to the membrane containing the chromosome III fragments (e.g., Figure 1B, left). The hybridization signal for each fragment was determined. Then, to permit ready comparisons among different experiments, the hybridization signal for each fragment was expressed as a fraction of the sum of the signals from all fragments on the same filter. As a control for variations in hybridization intensity unrelated to the ChIP enrichment, a sample of sheared DNA was removed prior to immunoprecipitation, labeled, and hybridized in parallel with the ChIP sample to an identical filter (e.g., Figure 1B, right), with results again expressed as fractional hybridization signals. For each fragment, the final relative abundance of protein-bound DNA was obtained by dividing the normalized ChIP signal by the corresponding normalized hybridization signal in the control sample.

The data obtained by such analysis for the cohesin protein Mcd1/Scc1 (triple HA-tagged) in an asynchronous culture are presented at high and low resolution in Figures 1C and Figure 2A. The pattern of relative abundance of Mcd1/Scc1 comprises a series of peaks and valleys of hybridization intensity along the chromosome, reflecting local maxima and minima. The average abundance for the whole chromosome is indicated by an abundance value of 1. Because of the way the data are normalized, the depths of the valleys, even in cases where no binding occurs, are limited by the level of

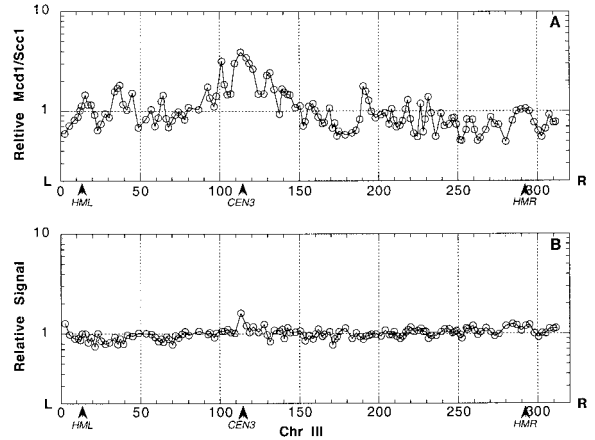


Figure 2. The Relative Distribution of Mcd1/Scc1 and Mock-Immunoprecipitated DNA in a Logarithmic Culture

For convenience every fragment is represented by its midpoint, and the points are connected. (A) Mcd1/Scc1. (B) Signals generated by a mock immunoprecipitation sample obtained from a culture of an isogenic strain lacking the MCD1/SCC1 terminal tag (YBY3).

nonspecific background (i.e., DNA that is immunoprecipitated via nonspecific associations with the agarose beads used for immunoprecipitation). For example, in the control experiment shown in Figure 2B, total signal intensity, normalized to the number of cells used, was 20% of the total ChIP signal obtained with the tagged Mcd1/Scc1. Correspondingly, the theoretical minimal value for the signal (i.e., the possibly lowest value for a valley) is 0.2, assuming that the intensity of hybridization signals is proportional to the amount of DNA used as a probe. Nonspecific background will also tend to decrease the peaks (by increasing the sum of signals). Thus, for two reasons, the actual differences in signal intensity between peaks and valleys are somewhat greater than they appear.

Control experiments establish that the differences observed in this analysis represent bona fide signals corresponding to Mcd1/Scc1 localization. First, when the standard procedure was performed on an isogenic strain expressing no tagged protein, the hybridization signals were essentially identical to those obtained from the total DNA control sample (1 ± 0.12 , Figure 2B). Thus, enrichment for a specific sequence in our assay can result only from binding to the immunoprecipitated protein. Residual variation of signal in the no-tag control experiments reflects small fluctuations in both the hybridization signal and nonspecific background (i.e., counts not specifically associated with the DNA spots). Second, the relative abundance signals revealed by this type of experiment are highly reproducible from experiment to experiment. Average standard deviations were 10.5% and 7.7% of the signals for Mcd1/Scc1 and Smc1, respectively ($n = 2$). Moreover, exactly the same peaks and valleys are observed among independent experiments (e.g., the three shown in Figures 3A–3C, discussed below). Third, the same distribution as that observed with HA-tagged protein in the SK1 strain background, with essentially the same peaks, is obtained with an 18-Myc-tagged version of Mcd1/Scc1 in

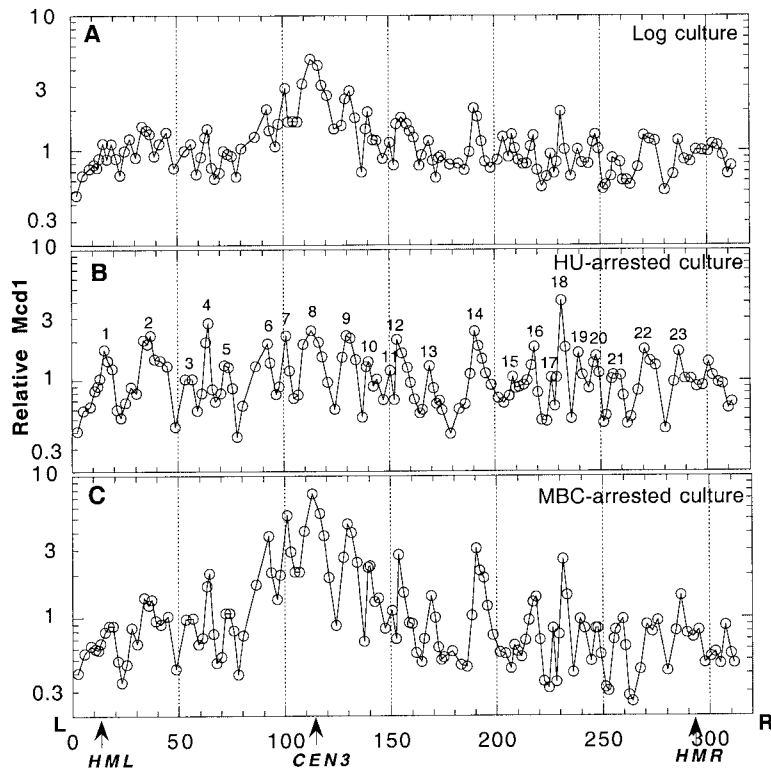


Figure 3. Relative Distribution of Mcd1/Sccl in Cycling Cells and Cells Arrested at Early S or G2/M

Cultures of cycling K6565 cells and HU or MBC arrested cells (arrest was verified by FACS analysis) was processed through ChIP and hybridization, and relative abundance of Mcd1/Sccl was determined. For making comparison convenient, every fragment is represented by its midpoint, and points are connected by lines.

a different genetic background (W303, Figure 3A). The patterns for the two strains did differ consistently in a few places. Those places were usually in close proximity to the sites of documented sequence differences between the two strain backgrounds (e.g., Ty element insertions or excisions, Figure 1C). Fourth, signal intensity varies directly with the abundance of the sequence in the sample as shown by the fact that fragments containing repetitive sequences such as Ty elements give much more intense signals in the total DNA control hybridization than do other fragments along the chromosome (e.g., Figure 1B).

Analysis of Mcd1/Sccl Distribution along Chromosome III of an Asynchronous Cell Population

The distribution of Mcd1/Sccl-bound DNA oscillates along the length of the chromosome as an alternating series of peaks and valleys (Figures 2A and 3). This pattern implies that Mcd1/Sccl is bound preferentially to certain particular positions along the chromosome. A total of ~23 signal peaks can be defined, as seen most easily in arrested cell cultures discussed below (Figure 3B). Each of these peaks consisted of 1–3 fragments. With the exception of peaks number 12 and 23, all the peaks were observed in each of the four experiments shown in Figures 2 and 3.

In all cases the signals are not represented by sharp spikes in hybridization but rather by relatively broad peaks and valleys each of which usually spans several adjacent test fragments. It is possible that this feature reflects a smooth variation of cohesin binding along the chromosome. On the other hand, it cannot be excluded that cohesin is bound uniquely to the fragments corresponding to the signal peaks, because the methodology

itself will tend to produce this type of pattern even in the case of binding restricted to a short DNA sequence. Spreading of the signal can arise due to the terminal overlap in sequence among filter-bound fragments (above) and/or because a fraction of sheared fragments will contain sequences contained in fragments adjacent to that containing an actual binding site. Nonetheless, some of the ~23 peaks comprise more than three fragments and thus span a distance (from valley to valley) greater than can be accounted for by the overlap between the filter-bound fragments or extra long sheared fragments. Thus, the possibility that Mcd1/Sccl binding spreads outward from the primary binding sites remains open.

Additionally, the heights of both peaks and valleys appear to vary coordinately in different segments of the chromosome. Peak height in a ~50 kb pericentric region that comprises about five major peaks is much higher than 1, which represents the average value for the whole chromosome. Indeed, the fragment that exhibits the single highest signal in this analysis is the one containing *CEN3*. Signals in the arm regions nearest the centromere fluctuate around 1, while those in the centromere-distal half of the right arm fluctuate around slightly less than one. Signals also appear to be descending toward both the right and the left ends of the chromosome.

It should be noted that the distribution observed reflects a population average of different cells at the same and different stages of the cell cycle (Discussion).

Mcd1/Sccl Distribution in Cell Cycle-Arrested Cultures

To investigate the Mcd1/Sccl distribution at different cell cycle stages, duplicate portions of a single logarithmically growing culture were treated with hydroxyurea

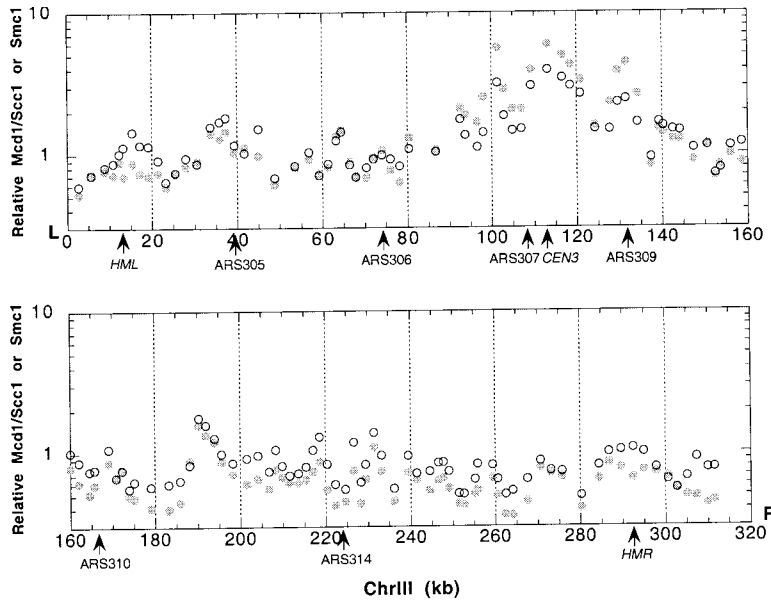


Figure 4. The Correlation between Mcd1/Scc1 and Smc1 Distribution
Relative abundance of Mcd1/Scc1 (open circles) and Smc1 (closed circles) as determined in cycling cultures of YBY92 and YBY84, respectively. Every fragment is represented by its midpoint.

(HU), which blocks cells in early S phase, or the microtubule depolymerizing agent MBC, which arrests cells in G2/M. Following 3 hr incubation, the two cultures were processed in parallel through ChIP and hybridization procedures. Individual peaks of Mcd1/Scc1 signal were at almost identical positions in both cultures as in asynchronously dividing cultures (compare Figures 3B and 3C with Figure 3A). In the MBC-arrested culture, peaks and valleys in and around the centromere were much higher than along the arms, with signals fluctuating around a value substantially higher than 1. In the HU-arrested culture, in contrast, all of the peaks are of similar height, as are all of the valleys, and both features fluctuate relatively evenly around the mean value (1) along the entire chromosome. The left terminus, and to a lesser extent the right terminus, are depleted for Mcd1/Scc1 binding in all situations, however.

The cohesin distribution of the MBC-arrested culture could differ from that of the HU-arrested culture either by the presence of more bound Mcd1/Scc1 in the centric region and/or by a deficit of bound protein along the chromosome arms. The latter possibility seems to be in accord with two other observations. First, the total amount of hybridization signal obtained from HU-arrested cultures was 1.4 \times and 3.9 \times higher than that obtained from the MBC-arrested cultures in the cases of poly Myc-tagged Mcd1/Scc1 and HA-tagged Smc1 (which behaves analogously, see below), respectively. Second, in cycling cells, Mcd1/Scc1 levels are lower at G2/M than at S phase, when cohesin levels are at their maximum (Guacci et al., 1997).

The distribution of Mcd1/Scc1 in the logarithmic culture (Figure 3A) resembles, qualitatively, the MBC arrest distribution in that centric region sites are again more prominently represented than arm sites. Thus, the presence of large amounts of Mcd1/Scc1 in an extended region around the centromere occurs during a significant portion of the normal cell cycle. The amplitude of the variation between peaks and valleys is lower in the asynchronous culture than the MBC-treated culture, however. This difference can be explained if a significant

portion of the cells in the asynchronous culture have their chromosome III's either in the HU arrest distribution or lack cohesin binding altogether (e.g., are in telophase-early G1). (The relative contributions of the two alternative configurations cannot be determined, as they have similar qualitative effects on relative peak heights).

The Distribution of Smc1 along the Chromosome

Localization of Mcd1/Scc1 to chromosomes depends upon another component of the cohesin complex, Smc1 (Michaelis et al., 1997; Toth et al., 1999). We applied the protocol described above to a logarithmically growing culture of a strain carrying a triple-HA, C-terminally tagged version of Smc1. The pattern of Smc1 distribution along chromosome III is essentially the same as that of Mcd1/Scc1, with the same peaks and valleys observed in both cases (Figure 4). Minor differences, for example, a tendency for peaks in certain regions to be systematically slightly higher or slightly lower, likely reflect minor differences in the relative distributions of cells among different cell cycle stages in the two cultures rather than true differences in cohesin binding. Moreover, exactly like Mcd1/Scc1, Smc1 was more abundant around the centromere in MBC-arrested cultures and partitioned more equally throughout the chromosome when the culture was arrested at early S phase by HU (data not shown).

Correlation between Mcd1/Scc1 Distribution and DNA Composition

Smc proteins preferentially bind AT-rich DNA (Akmedov et al., 1998). For these reasons, and others, we examined the relationship between the pattern of peaks and valleys in the cohesin distribution and variations in base composition along chromosome III. All yeast chromosomes, including chromosome III, exhibit broad regional biases comprising GC-rich and AT-rich isochores that average around 50 kb (e.g., Figure 5A; Sharp and Lloyd, 1993; Dujon, 1996), which may correspond to the mammalian R bands and G bands (Discussion). The distribution of cohesins does not correlate with

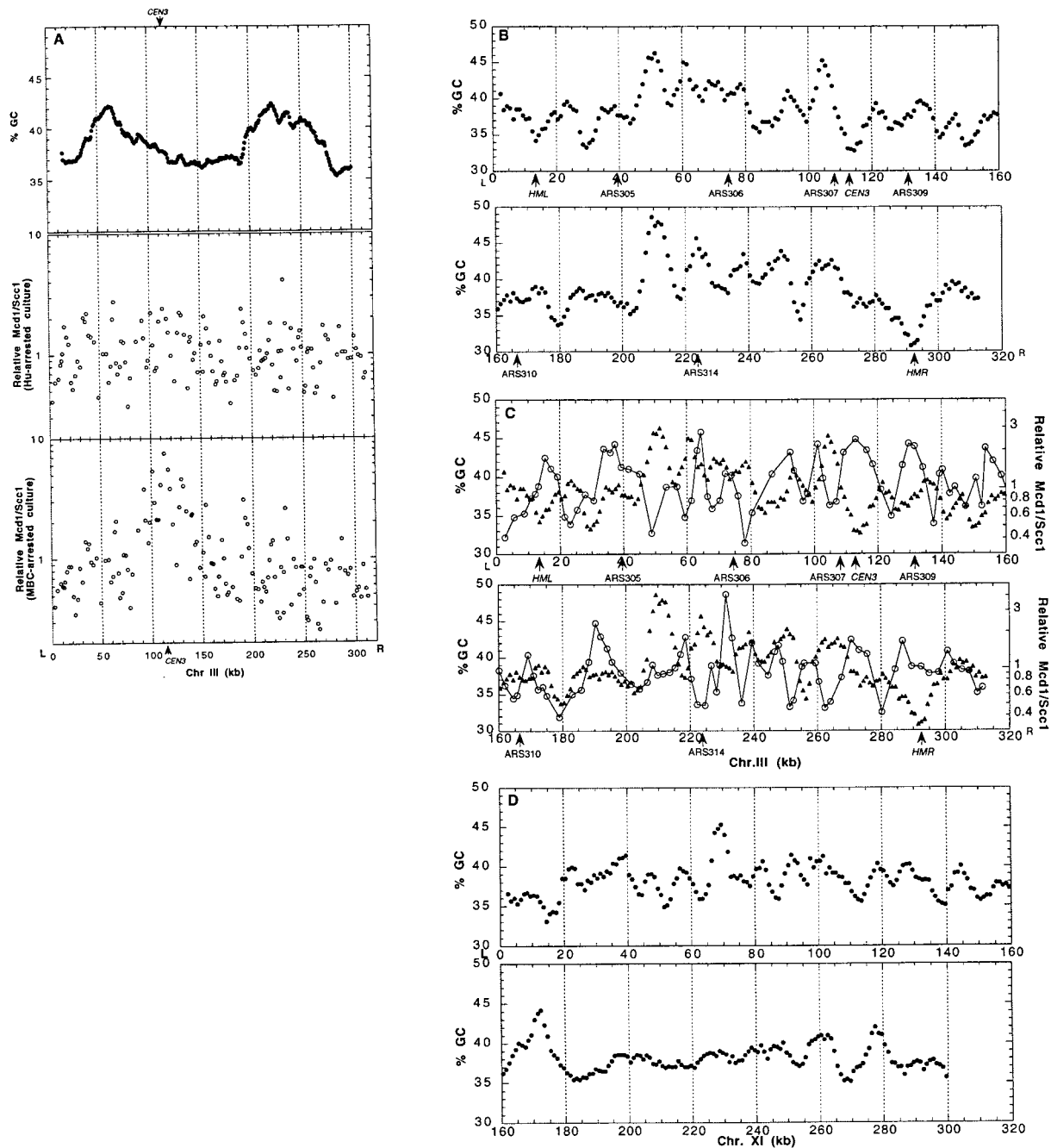


Figure 5. The Correlation between Mcd1/Sccl1 Distribution and Base Composition

(A) Base composition isochores in chromosome III as illustrated by a sliding window of 30 kb and compared with the distribution of Mcd1/Sccl1 during early S phase or G2/M (the data are taken from Figure 3).

(B) Local fluctuations in base composition in chromosome III revealed by a sliding window of 5 kb.

(C) The correlation between oscillations local base composition (triangles) and Mcd1/Sccl1 distribution (open circles) at early S phase. (The data are taken from Figure 3.)

(D) Local fluctuations in base composition in the left arm of chromosome XI revealed by a sliding window of 5 kb.

these isochores (Figure 5A). The HU arrest distribution is essentially even across the chromosome at this level of resolution. The MBC arrest distribution is also clearly different from the isochore pattern; for example, the centromeric region overlaps with parts of both GC- and AT-rich domains.

The pattern of cohesin binding revealed by this work

is suggestive of preferred binding (or nucleation) sites that occur, on average, once per ~ 13 kb along the chromosome. We therefore investigated the possibility that base composition might also fluctuate regularly along the chromosome with a second, smaller periodicity. The presence of isochores is revealed by analysis of base composition with a sliding window of 30–50 kb (e.g.,

Dujon, 1996). We carried out an analogous analysis using progressively smaller sliding windows. As the size of the window decreases to 10 kb or less, a new type of base composition oscillation is revealed. These more local fluctuations are characterized by an average periodicity of ~ 15 kb. This pattern is most pronounced with a sliding window of 5 kb (Figure 5B) but is apparent at window sizes as high as 10 kb and as low as 1 kb.

Moreover, peaks of Mcd1/Scs1 binding appear, by inspection, to correlate closely with the peaks of high local AT composition; Mcd1/Scs1 appears to occur preferentially in regions that are locally AT rich, while, in complementary fashion, locally GC-rich regions were usually depleted for Mcd1/Scs1 (Figure 5C). This correlation can be verified statistically. Fragments were sorted into two sets according to whether they are enriched or depleted for Mcd1/Scs1 relative to the average (i.e., giving signals of >1 or <1 , respectively); the average base compositions for the two sets differed by 1.6% ($61.37\% \pm 2.94\%$ AT and $59.79\% \pm 3.88\%$ AT, respectively). An even larger difference was observed between the set of fragments representing the 23 peaks of cohesin binding and the set representing the intervening valleys ($61.2\% \pm 3.09\%$ AT and $58.78\% \pm 3.97\%$ AT, respectively). Both differences are statistically significant ($p < 0.005$ by Student's *t* test). Nevertheless, not every locally AT-rich peak was enriched with Mcd1/Scs1 (e.g., those centered at ~ 30 kb and ~ 180 kb; Figure 5C), and, conversely, some regions that showed enrichment for Mcd1/Scs1 were not AT rich (e.g., ~ 34 – 38 kb; Figure 5C). We infer that while cohesin binding is closely correlated with overall AT composition, this is not the only relevant factor. Other proteins might either favor or disfavor utilization of preferred binding sequences; also, a small AT-rich sequence might sometimes provide a strong binding site even in a region that, globally, is GC rich.

We have also analyzed base composition in chromosome XI using a 5 kb sliding window. The results (shown only for the telomere-proximal 300 kb of the left arm, Figure 5D) suggest that the ~ 15 kb fluctuations in base composition are a general characteristic of yeast chromosomes. Again, however, the oscillation pattern breaks down in certain short regions (e.g., 185–195 kb [Figure 5B] and 200–250 kb [Figure 5D]).

We also attempted to determine whether a specific consensus sequence element responsible for cohesin binding could be identified. First, a set of several fragments in which binding could be confined to a short, 1–2 kb region (Figure 1C) were analyzed by several multiple and pairwise alignment programs to search for a common sequence element that localizes to the sites enriched for Mcd1/Scs1 along the whole chromosome. No such element could be identified. The large nature of the test fragments would have precluded identification of any relatively short, potentially degenerate binding motif, however, leaving open the possibility that such an element exists. Second, taking into consideration the correlation between base composition and cohesin distribution, we attempted to examine whether more specific AT-rich motifs, specifically characteristic of scaffold attachment sites (SARs) in *Drosophila*, correlate better than base composition with the pattern of Mcd1/Scs1 distribution. None of the motifs tested, including

AATAAAT/CAAAA, TTA/TTA/TTTA/TTT, and other more redundant motifs (Gasser and Laemmli, 1986; Amati et al., 1990), satisfied this criterion.

Discussion

Cohesins Bind Preferentially at Particular Genetically Determined Sites along the Chromosome

The distribution patterns exhibited by Mcd1/Scs1 and Smc1-bound DNA suggest that both proteins occur preferentially at the same ~ 23 locations along yeast chromosome III. This pattern likely reflects the positions of the corresponding cohesin complexes. Since the positions of the binding peaks are correlated with underlying base composition, they are presumably determined by the underlying DNA sequence, either directly (e.g., via the Smc proteins, which are known to bind AT-rich sequences preferentially; Akhmedov et al., 1998) or indirectly (e.g., via association of cohesins with other axis-associated components). Each peak may represent a single unique consensus binding determinant or a cluster of such determinant. It is unclear whether cohesins also bind at lower probability, within flanking fragments, either via additional binding sites or by nucleation from sites in the peak fragments.

The predicted total number of cohesin-binding sites in the entire yeast genome, given ~ 23 per 315 kb of chromosome III, is approximately 1000. Immunocytological studies, however, report a maximum of ~ 100 Mcd1 foci (Michaelis et al., 1997) and ~ 100 foci of the *S. pombe* Mcd1/Scs1 homolog Rec8 in meiotic prophase cells (Parisi et al., 1999). Thus, a given chromosome in a given nucleus may assemble cohesin complexes on only a subset of the potential preferred binding sites, with the ChIP distribution representing the population average of all configurations. Alternatively, immunostaining foci might represent clusters of binding sites ("rosettes") or the $\sim 10\%$ of sites per nucleus that contain an above-threshold level of protein.

Interestingly, a study of the effects of sequential, large deletions on the stability of chromosome III revealed progressive reduction in stability as the size of the chromosome decreased, with accelerated reduction in stability below 100 kb (Surosky et al., 1986). Progressive deletion of cohesin-binding sites could account for this observation. Conversely, difficulty in identifying specific noncentric sites involved in sister segregation may be explained by occurrence of cohesin-binding sites every ~ 13 kb.

The Pattern of Cohesin Abundance along the Chromosome

A region of ~ 50 kb around the centromere is highly enriched for Mcd1/Scs1 and Smc1 in asynchronous cultures. It seems probable that the prominence of cohesins in centric regions versus arm regions plays a role in the differential behavior of sister connections in the two regions during mitotic and meiotic chromosome segregation (Introduction).

In HU-arrested cells, however, the heights of cohesin binding peaks are relatively similar along both arms and centric regions. Since cohesins first appear on the chromosomes of normally cycling cells prior to, or at the

beginning of, S phase (Michaelis et al., 1997), and assuming that the HU-arrested culture represents the corresponding point in the normal cell cycle, these findings suggest that cohesin distribution changes during the cell cycle. Cohesins would first appear on the chromosomes in the more even distribution and then, at some later stage, undergo a transition to a centric-biased distribution. Furthermore, the uneven cohesin distribution appears to arise by depletion of cohesins from the arm regions.

A centromere-biased distribution might arise either (a) prior to the onset of sister separation at metaphase/anaphase or (b) at and after this point, concomitant with loss of sister chromatid cohesion. In the first case, a biased distribution could arise as part of the replication-linked establishment of sister chromatid connections during S phase or, alternatively, after establishment of cohesion as a "minimization" process that occurs along the arms during subsequent chromosome morphogenesis (e.g., during the onset of higher order compaction) (Kleckner, 1996; van Heemst et al., 1999 [this issue of *Cell*]) or during loop formation (Introduction). In the second case, an HU arrest distribution of cohesins would be present during late G1, S, and G2; a biased configuration might then arise at the metaphase/anaphase (M/A) transition, beginning with a distribution like that observed in MBC-arrested cells, and possibly followed by complete loss of cohesins along the arms during anaphase (A). We favor establishment of a biased distribution prior to M/A. Since the period encompassing M/A-A is very short as compared to that occupied by G1/S/G2 (e.g., ~10% versus ~90%; Table 11 in Yamamoto et al., 1996), it is problematical that the degree of centric bias observed in asynchronous cultures could reflect the presence of bias only during the segregation process. The fact that sister chromatids are not widely separated in MBC-arrested cells (Guacci et al., 1994) would also be consistent with establishment of centric bias prior to M/A. On the other hand, MBC-arrested cells might have undergone some diminution in the robustness of sister chromatid cohesion not detectable by FISH.

In HU-arrested cells, where only a few kilobases of DNA can be replicated (and only from early origins) (Santocanale and Diffley, 1998), many cohesin peaks are quite far from origins of replication (e.g., Figures 5C) and thus must represent unreplicated DNA. More generally, there is no correlation between replication origins and cohesin binding peaks. This implies that replication-linked establishment of sister connectedness might arise during the elongation phase of replication, or at the positions of colliding or stalling replication forks, rather than during the initiation phase.

Cohesin Abundance Reflects Specialized Organization in Centric Regions and Chromosome Ends

Genetic studies define a minimal yeast centromeric segment of 125 bp. Cohesin binding is more abundant, however, in a broad ~50 kb zone centered on minimal *CEN3*. *S. cerevisiae* centromeres may thus be structurally analogous to eukaryotic centromeres, which comprise DNA segments of 40–100 kb in *S. pombe*, or more in higher eukaryotes, and usually contain repetitive elements (reviewed in Karpen and Allshire, 1997; Murphy

and Karpen, 1998). Conversely, the current findings suggest that the broad centromeric structure observed in larger organisms may play its role in sister chromatid cohesion via an increased abundance of cohesins. The special prominence of cohesin binding in centric regions might be conferred by consensus binding sites alone, by additional genetic determinants in these regions, and/or via spreading effects nucleated by the minimal *CEN3* region.

Oppositely, cohesins appear to be less abundant near chromosome III ends, in regions having a specialized, "silenced" chromosome structure. Since yeast chromosome ends are organizationally analogous to those of other eukaryotes (Pryde et al., 1997), this pattern may be evolutionarily general. Interestingly, two other silenced regions, *HML* and *HMR*, also exhibit lower cohesin abundance than expected from their AT composition and apparent scaffold association (Amati and Gasser, 1988). Cohesin abundance in telomeric repeat segments remains to be determined.

Two Types of Base Composition Variations with Distinct Correlations for Chromosome Organization and Function

Yeast chromosomes exhibit regional biases in average base composition, the GC- and AT-rich isochores, which are typically ~50 kb in length and represent a long-range base composition variation. These isochores may correspond to mammalian R and G bands as shown by similarities in base composition bias and gene density (Dujon, 1996). These isochores appear to have a functional significance in yeast, because hot spots for meiotically programmed double-strand breaks occur almost entirely in the GC-rich zones (Baudat and Nicolas, 1997). Similarly, perhaps, meiotic crossovers occur preferentially in R bands in both mouse and human (Holmquist, 1992).

The current work reveals that average base composition along yeast chromosomes also exhibits a second, "short-range" fluctuation: local average base composition oscillates between AT-rich peaks and AT-poor (GC-rich) valleys with a rather regular periodicity of ~15 kb. Its regularity, plus its correlation with cohesin binding distribution, suggests that this feature is functionally significant. Since mitotic chromosome axes are thought to arise via the protein-mediated coalescence of AT-rich regions (Saitoh and Laemmli, 1993; Swedlow and Hirano, 1996), AT-rich peaks should promote periodic localization of certain sequences to the chromosome axis/scaffold (i.e., to generate arrays of loops via an AT-queue) (Saitoh and Laemmli, 1993). The average size of a yeast chromatin loop at meiotic pachytene, ~20 kb (Moens and Pearlman, 1988), is slightly larger than the average spacing of AT-rich peaks. This may suggest that only a subset of the potential sites is used in any given meiotic nucleus.

The long-range and short-range base composition biases are apparently superimposed upon one another (compare Figure 5A to Figure 5B). This opens the intriguing possibility that chromosome organization, structural and functional, might be determined by a combinatorial process involving interplay between both

elements, with additional inputs from more specific determinants such as centromeres and telomeres. Cohesins appear to respond only to the short-range fluctuations; other chromosome structure proteins might respond only to isochores or to both determinants.

Spatial Relationship of Bound Cohesins to the Chromosome Axes

It has been suggested that sister connections (Kleckner, 1996) or cohesins or cohesin complexes (Gasser, 1995; Guacci et al., 1997; Hirano, 1998; Jessberger et al., 1998) might occur preferentially at or near chromosome axes/scaffolds, at or along the bases of loops, and the possibility of a "supraaxial" position has been raised for the cohesion-implicated Spo76 protein (van Heemst et al., 1999). The correlation of cohesin binding with short-range fluctuations in AT composition and the presence of preferred cohesin-binding sites in regions preferentially enriched in scaffold fractions provide support for such possibilities. Furthermore, immunocytological studies demonstrate localization of cohesins to the axes of meiotic pachytene yeast chromosomes, independent of synapsis, also consistent with this possibility (Klein et al., 1999; J. Dekker, personal communication).

Applications and Extensions of the Experimental Approach

We have found the method described above applicable to other mitotic and meiotic chromosome structure proteins and to Orc1 (Y. B. and N. K., unpublished data), which is more specific in its localization as already shown by standard ChIP analysis (Aparicio et al., 1997). Our method should also be applicable to proteins that are very specific in their binding (e.g., transcription factors). Furthermore, the methodology should directly accommodate DNA fragment arrays bound to microchips or glass slides and thus be useful for genome-wide analysis of chromosome-associated proteins not only in yeast but also in other organisms.

Application of this approach to other cases will be limited by several factors. The number of cells processed must be large enough to generate a sufficient amount of immunoprecipitated DNA, which in turn depends upon the intrinsic binding level and the intimacy of binding for the protein of interest. Furthermore, the level of experimental noise must be kept to a minimum. In the case of organisms with larger genomes, potential noise may be increased due to the complexity of the genomes.

Our experimental system also is limited in its resolution. In the current study, resolution cannot exceed 1–3 kb, which reduces the potential for specific localization of discrete binding sites within a preferred membrane-bound fragment. Resolution can be improved somewhat by using smaller substrate fragments, though the gain from such an alteration is limited by the size and heterogeneity of the DNA fragments subjected to chromatin immunoprecipitation (100–2000 bp). A unique binding site could be identified, however, using a nested series of partially overlapping membrane fragments and/or by fragmentation of ChIP DNA by restriction enzyme cleavage rather than sonication.

As more proteins are analyzed by this method, in combination with genetic manipulation and genomic analysis, a more complete picture of functional domains and determinants of chromosomes and the interrelationships among different functions should emerge.

Experimental Procedures

Strains

The strain carrying an 18X Myc-tagged *MCD1/SCC1* was K6565 (Michaelis et al., 1997). All other strains are derived from SK1 derivative YBY3 (*MATa*, *ho::HISG*, *lys2*, *leu::HISG*, *arg4-bgl*, and *ura3*, *GAL*), an SK1 derivative. YBY84 and YBY92 carry triple-HA, C-terminal, tagged versions of *SMC1* and *MCD1/SCC1*, respectively, substituted for the corresponding wild-type genes via an accompanying KanMX marker. YBY98 is a diploid strain homozygous to all the markers carried by YBY92 except for heterozygosity at the *arg4* locus (*arg4-bgl/arg4-nsp*).

ChIP Analysis

The following information, plus additional details and primary data from several experiments, is available on the website <<http://mcb.harvard.edu/kleckner/ChIP.html>>.

Generation of Filters Containing the Chromosome III Fragments

The 133 analyzed fragments were generated by PCR with chromosomal DNA of YBY3 as DNA source. One hundred twenty-four were generated using "GenePairs primers" (Research Genetics Inc.); nine were generated with other primers. PCR products were run on agarose gels. Bands corresponding to the expected fragment size (always the major product) were cut and purified by a gel purification kit (either Bio101 or Qiagen). Purified fragments (2 ng each) were spotted on a positively charged membrane (Hybond-N+, Amersham) using a multiblot replicator (vp384S, VandP Scientific).

Chromatin Immunoprecipitation

The chromatin immunoprecipitation procedure is based on a previously described protocol (Hecht et al., 1996) with several modifications required for scaling up the procedure. Typically, an overnight culture was diluted 1/15 into YPD (2% peptone, 1% yeast extract, and 2% glucose). Cells were grown at 30°C until an O.D.₆₀₀ of 1–1.5 was reached. Aliquots of 0.6–1 l of cells were either cross-linked immediately or incubated for an additional 2.5–3 hr with either hydroxyurea (HU, 100 mM) or methyl 2-benzimidazolecarbamate (MBC, 80 μg/ml). Cross-linking was carried out by addition of formaldehyde (1%) followed by incubation, with occasional mixing, at room temperature, for 30 min. Cross-linking was terminated by the addition of 50 mM Tris-HCl (pH 7.5), and the cells were washed twice with 20 mM Tris-HCl, 150 mM NaCl. Cells were then resuspended in 8–15 ml of lysis buffer (50 mM HEPES/KOH [pH 7.5], 140 mM NaCl, 1 mM EDTA, 1% Triton X-100, 0.1% sodium deoxycholate) containing protease inhibitor mix (1 μg/ml leupeptin, 1 μg/ml pepstatinA, 1 μg/ml chemostatin, and 1 mM PMSF) and 0.4 mM Pefabloc (Boehringer Mannheim). Glass beads (425–600 μm, acid washed, Sigma) were then added, and the cells were lysed by vortexing for 40 min at 4°C. Unlysed cells and lysate were collected by centrifugation of the glass bead mix through a 30 ml syringe. Supernatant was collected and the pellet was resuspended in 5–8 ml of lysis buffer, containing protease inhibitors, and subjected to an additional 30 min of glass bead-mediated lysis. The pellet and supernatant were recovered by centrifugation, and the pellet was resuspended and combined with the supernatant from the first round of lysis. DNA was sheared by sonicating the suspension, on ice, four times for 15 s, using a Branson model W185 sonicator on setting 5. Unlysed cells and other cellular debris were removed by centrifugation for 5 min at 17,000 g followed by additional centrifugation for 10 min. After a 50 μl total DNA sample was removed, the cleared, sheared DNA lysate was used for immunoprecipitation. HA-tagged proteins were immunoprecipitated by incubating the lysate with 125 μg of anti-HA (12CA5, Boehringer Mannheim) for 1.5 hr at 4°C, followed by the addition of 70 μl of protein G agarose (Boehringer Mannheim) and incubating overnight. Myc-tagged proteins were immunoprecipitated by incubation with 50 μl of anti c-Myc agarose conjugate (9E10, Santa Cruz Biotech.) overnight. The beads were then washed

with 25 ml of lysis buffer containing protease inhibitor mix (twice), lysis buffer + 500 mM NaCl (once), 10 mM Tris-HCl (pH 8.0), 0.25 M LiCl, 0.5% NP-40, 0.5% sodium deoxycholate, and 1 mM EDTA (once) and finally with TE (10 mM Tris-HCl [pH 8.0] and 1 mM EDTA). Bound complexes were eluted by addition of 100 μ l of 50 mM Tris (pH 8.0), 10 mM EDTA, and 1% SDS followed by incubation at 65°C for 15 min and 1 min of centrifugation in mini centrifuge. After collection of the supernatant, 150 μ l of TE containing 0.67% SDS was added, beads were incubated at 65°C for 5 min, and the supernatant was collected after centrifugation and combined with the supernatant from the first elution step. The eluted complexes as well as the total DNA samples (after addition of 200 μ l of TE + 1% SDS) were incubated overnight at 65°C to reverse cross-linking. After cross-linking reversal, 250 μ l of TE containing 0.4 mg/ml proteinase K and 20 μ g/ml glycogen was added. Proteolysis was allowed to proceed for 3 hr at 37°C and then 55 μ l of 4 M LiCl was added, the samples were phenol-chloroform extracted, and DNA was precipitated with 2 vol of ethanol and washed with 75% ethanol. The immunoprecipitated DNA was resuspended in 10 μ l of 10 mM Tris-HCl (pH 8.0) and 0.1 mM EDTA containing 10 μ g/ml RNAaseA and incubated for 1 hr at 37°C. Total DNA samples were resuspended in 50 μ l of the same solution containing 200 μ g/ml RNAaseA and incubated as above.

Hybridization and Quantitation

Immunoprecipitated DNA (2–5 μ l) and total DNA (25 ng) were radiolabeled by a random priming kit (Stratagene). The labeled DNA was used to probe the membranes containing the chromosome III fragments, using ExpressHyb hybridization solution (Clontech), in the presence of 100 μ g/ml sheared salmon sperm DNA. Signal intensity for each fragments was quantified using a PhosphorImager.

Acknowledgments

We thank Kim Nasmyth for strains. We are also grateful to Diana van Heemst and Denise Zickler, as well as Franz Klein and Kim Nasmyth, for communicating results prior to publication. Y. B. was supported by fellowships from Human Frontiers (LT-27/97) and Damon Runion-Walter Winchell Cancer Research Fund (DRG-1462). Research was supported by a National Institutes of Health grant RO1-GM44794 to N. K.

Received April 19, 1999; revised June 8, 1999.

References

- Akhmedov, A.T., Frei, C., Tsai-Pflugfelder, M., Kemper, B., Gasser, S.M., and Jessberger, R. (1998). Structural maintenance of chromosomes protein C-terminal domains bind preferentially to DNA with secondary structure. *J. Biol. Chem.* **273**, 24088–24094.
- Amati, B.B., and Gasser, S.M. (1988). Chromosomal ARS and CEN elements bind specifically to the yeast nuclear scaffold. *Cell* **54**, 967–978.
- Amati, B., Pick, L., Laroche, T., and Gasser, S.M. (1990). Nuclear scaffold attachment stimulates, but is not essential for ARS activity in *Saccharomyces cerevisiae*: analysis of the *Drosophila*-ftz SAR. *EMBO J.* **9**, 4007–4016.
- Aparicio, O.M., Weinstein, D.M., and Bell, S.P. (1997). Components and dynamics of DNA replication complexes in *S cerevisiae*: redistribution of MCM proteins and Cdc45p during S phase. *Cell* **91**, 59–69.
- Bajer, A.S., and Mole-Bayer, J. (1972). *Spindle Dynamics and Chromosome Movements* (New York: Academic Press).
- Baudat, F., and Nicolas, A. (1997). Clustering of meiotic double-strand breaks on yeast chromosome III. *Proc. Natl. Acad. Sci. USA* **94**, 5213–5218.
- Biggins, S., and Murray, A.W. (1998). Sister chromatid cohesion in mitosis. *Curr. Opin. Cell Biol.* **10**, 769–775.
- Birkenbihl, R.P., and Subramani, S. (1995). The RAD21 gene-product of *Schizosaccharomyces pombe* is a nuclear, cell-cycle-regulated phosphoprotein. *J. Biol. Chem.* **270**, 7703–7711.
- DeRisi, J.L., Iyer, V.R., and Brown, P.O. (1997). Exploring the metabolic and genetic control of gene expression on a genomic scale. *Science* **278**, 680–686.
- Dujon, B. (1996). The yeast genome project: what did we learn? *Trends Genet.* **12**, 263–270.
- Furuya, K., Takahashi, K., and Yanagida, M. (1998). Faithful anaphase is ensured by Mis4, a sister chromatid cohesion molecule required in S phase and not destroyed in G1 phase. *Genes Dev.* **12**, 3408–3418.
- Gasser, S.M. (1995). Coiling up chromosomes. *Curr. Biol.* **5**, 357–360.
- Gasser, S.M., and Laemmli, U.K. (1986). Cohabitation of scaffold binding regions with upstream/enhancer elements of three developmentally regulated genes of *D. melanogaster*. *Cell* **46**, 521–530.
- Guacci, V., Hogan, E., and Koshland, D. (1994). Chromosome condensation and sister-chromatid pairing in budding yeast. *J. Cell Biol.* **125**, 517–530.
- Guacci, V., Koshland, D., and Strunnikov, A. (1997). A direct link between sister chromatid cohesion and chromosome condensation revealed through the analysis of MCD1 in *S. cerevisiae*. *Cell* **91**, 47–57.
- Hecht, A., Strahl-Bolsinger, S., and Grunstein, M. (1996). Spreading of transcriptional repressor SIR3 from telomeric heterochromatin. *Nature* **383**, 92–96.
- Hirano, T. (1995). Biochemical and genetic dissection of mitotic chromosome condensation. *Trends Biochem. Sci.* **20**, 357–361.
- Hirano, T. (1998). SMC protein complexes and higher-order chromosome dynamics. *Curr. Opin. Cell Biol.* **10**, 317–322.
- Holmquist, G.P. (1992). Chromosome bands, their chromatin flavors, and their functional features. *Am. J. Hum. Genet.* **51**, 17–37.
- Jessberger, R., Frei, C., and Gasser, S.M. (1998). Chromosome dynamics: the SMC protein family. *Curr. Opin. Genet. Dev.* **8**, 254–259.
- Karpen, G.H., and Allshire, R.C. (1997). The case for epigenetic effects on centromere identity and function. *Trends Genet.* **13**, 489–496.
- Kleckner, N. (1996). Meiosis: how could it work? *Proc. Natl. Acad. Sci. USA* **93**, 8167–8174.
- Klein, F., Mahr, P., Galova, M., Buonomo, S.B.C., Michaelis, C., Nairz, K., and Nasmyth, K. (1999). A central role for cohesins in sister chromatid cohesion, formation of axial elements, and recombination during yeast meiosis. *Cell* **98**, 91–103.
- Losada, A., Hirano, M., and Hirano, T. (1998). Identification of Xenopus SMC protein complexes required for sister chromatid cohesion. *Genes Dev.* **12**, 1986–1997.
- Maguire, M.P. (1995). Is the synaptonemal complex a disjunction machine? *J. Hered.* **86**, 330–340.
- Michaelis, C., Ciosk, R., and Nasmyth, K. (1997). Cohesins: chromosomal proteins that prevent premature separation of sister chromatids. *Cell* **91**, 35–45.
- Miyazaki, W.Y., and Orr-Weaver, T.L. (1994). Sister-chromatid cohesion in mitosis and meiosis. *Annu. Rev. Genet.* **28**, 167–187.
- Moens, P.B., and Pearlman, R.E. (1988). Chromatin organization at meiosis. *Bioessays* **9**, 151–153.
- Mole-Bajer, J. (1958). Cine-micrographic analysis of c-mitosis in endosperm. *Chromosoma* **9**, 322–358.
- Murphy, T.D., and Karpen, G.H. (1998). Centromeres take flight: alpha satellite and the quest for the human centromere. *Cell* **93**, 317–320.
- Newlon, C.S., Collins, I., Dershowitz, A., Deshpande, A.M., Greenfeder, S.A., Ong, L.Y., and Theis, J.F. (1993). Analysis of replication origin function on chromosome III of *Saccharomyces cerevisiae*. *Cold Spring Harb. Symp. Quant. Biol.* **58**, 415–423.
- Nicklas, R.B. (1988). The forces that move chromosomes in mitosis. *Annu. Rev. Biophys. Chem.* **17**, 431–449.
- Parisi, S., McKay, M.J., Molnar, M., Thompson, M.A., van der Spek, P.J., van Druenen-Schoenmaker, E., Kanaar, R., Lehmann, E., Hoeymakers, J.H.J., and Kohli, J. (1999). Rec8p, a meiotic recombination and sister chromatid cohesion phosphoprotein of the Rad21p family, conserved from fission yeast to humans. *Mol. Cell Biol.* **19**, 3515–3528.
- Pryde, F.E., Gorham, H.C., and Louis, E.J. (1997). Chromosome ends: all the same under their caps. *Curr. Opin. Genet. Dev.* **7**, 822–828.

- Saitoh, Y., and Laemmli, U.K. (1993). From the chromosomal loops and the scaffold to the classic bands of metaphase chromosomes. *Cold Spring Harb. Symp. Quant. Biol.* *58*, 755–765.
- Santocanale, C., and Diffley, J.F. (1998). A Mec1- and Rad53-dependent checkpoint controls late-firing origins of DNA replication. *Nature* *395*, 615–618.
- Selig, S., Okumura, K., Ward, D.C., and Cedar, H. (1992). Delineation of DNA-replication time zones by fluorescence in situ hybridization. *EMBO J.* *11*, 1217–1225.
- Sharp, P.M., and Lloyd, A.T. (1993). Regional base composition variation along yeast chromosome III: evolution of chromosome primary structure. *Nucleic Acids Res.* *21*, 179–183.
- Skibbens, R.V., Corson, L.B., Koshland, D., and Hieter, P. (1999). Ctf7p is essential for sister chromatid cohesion and links mitotic chromosome structure to the DNA replication machinery. *Genes Dev.* *13*, 307–319.
- Strunnikov, A.V., Larionov, V.I., and Koshland, D. (1993). Smc1, an essential yeast gene encoding a putative head-rod-tail protein, is required for nuclear division and defines a new ubiquitous protein family. *J. Cell Biol.* *123*, 1635–1648.
- Sumner, A.T. (1991). Scanning electron-microscopy of mammalian chromosomes from prophase to telophase. *Chromosoma* *100*, 36–43.
- Surosky, R.T., Newlon, C.S., and Bik-Kwoon, T. (1986). The mitotic stability of deletion derivatives of chromosome III in yeast. *Proc. Natl. Acad. Sci. USA* *83*, 414–418.
- Swedlow, J.R., and Hirano, T. (1996). Chromosome dynamics: Fuzzy sequences, specific attachments? *Curr. Biol.* *6*, 544–547.
- Toth, A., Ciosk, R., Uhlmann, F., Galova, M., Schleiffer, A., and Nasmyth, K. (1999). Yeast cohesin complex requires a conserved protein, Eco1p(Ctf7), to establish cohesion between sister chromatids during DNA replication. *Genes Dev.* *13*, 320–333.
- Uhlmann, F., and Nasmyth, K. (1998). Cohesion between sister chromatids must be established during DNA replication. *Curr. Biol.* *8*, 1095–1101.
- van Heemst, D., James, F., Poggeler, S., Berteaux-Lecellier, V., and Zickler, D. (1999). Spo76p is a conserved chromosome morphogenesis protein that links the mitotic and meiotic programs. *Cell* *98*, this issue, 261–271.
- Yamamoto, A., Guacci, V., and Koshland, D. (1996). Pds1p is required for faithful execution of anaphase in the yeast, *Saccharomyces cerevisiae*. *J. Cell Biol.* *133*, 85–97.